EXPERIMENTAL AND THEORETICAL RESULTS ON THE ORBIT OF ECHO I[1]

by

Pedro E. Zadunaisky[2], Irwin I. Shapiro[3], and Harrison M. Jones[3]

In this report we compare experimental and theoretical determinations of the orbital elements of Satellite 1960 ζ 1 (Echo I) for every day from August 13, 1960 (one day after launching) through January 11, 1961. This comparison shows that the strikingly large variations of the eccentricity and the geocentric perigee distance are almost wholly attributable to the effects of sunlight pressure on the balloon; this conclusion is in accordance with our earlier theoretical predictions (Parkinson, Jones, and Shapiro, 1960; Shapiro and Jones, 1960).

We have also inferred atmospheric densities for the altitude range (about 950 to 1500 km above the International Ellipsoid) traversed by Echo. In this calculation it is necessary to consider the energy gain (or loss) of the satellite from the solar radiation. After subtracting the variations of the rate of change of period due to this latter effect, we find that the remaining fluctuations are strongly correlated with those of the solar flux at 10.7 cm and 20.0 cm wavelengths and can be attributed almost entirely to air drag. In addition, the air drag shows a large increase during the major solar flares of November and December.

From the time variation of eccentricity we deduced approximate values for the rate of gas leakage from the balloon. Our conclusions are only tentative because many other quantities of uncertain magnitudes (such as the solar constant, which we know only imprecisely) influence our results.

Our present best estimate of the lifetime of Echo I is that, barring a substantial change in its shape, it will perish in July 1963.

---

1 The present paper has been sent to the National Aeronautics and Space Administration as a contribution to NASA's general report on Satellite Echo I.

2 Smithsonian Astrophysical Observatory and Harvard College Observatory, Cambridge, Mass.

3 Lincoln Laboratory, M.I.T., Lexington, Mass., operated with support from the U.S. Air Force.

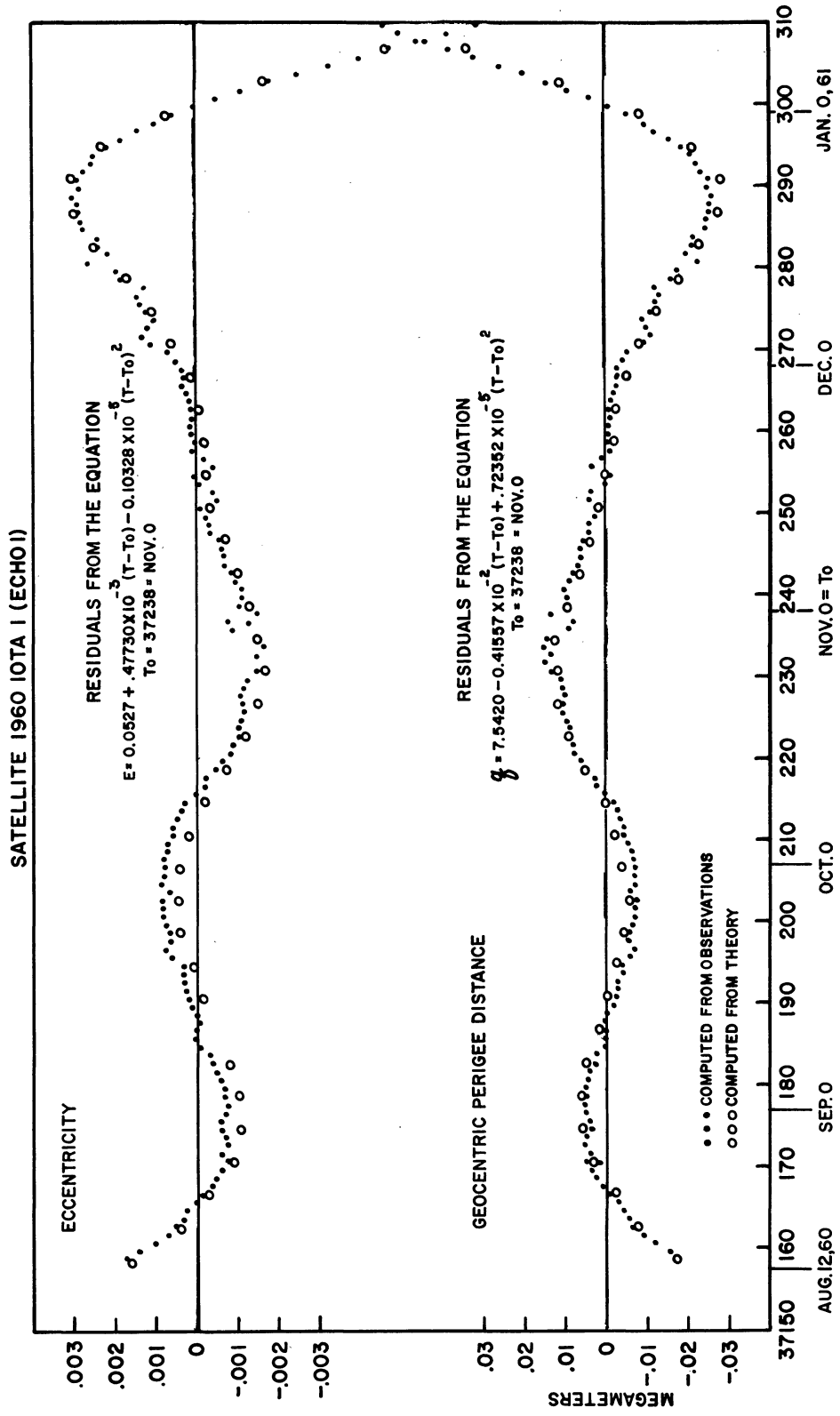

FIGURE 1. --Residuals of the values of the eccentricity and geocentric perigee distance with respect to polynomials obtained by least-squares fit.

1. Description of Experimental Orbit Computation

From observed positions of the satellite we have derived the mean orbital elements by a process of successive differential corrections. That process has already been described in detail (Zadunaisky, 1960), and therefore we shall give only the main features of the present computations.

The observations used came mainly from the Smithsonian Baker-Nunn photographic tracking stations. We also used some radio observations from the Minitrack stations of Goddard Space Flight Center for the time during which the satellite's beacon was operating, as well as a very large number of excellent optical observations from the Observatory of Paris at Meudon (France).

The word mean in reference to the orbital elements must be understood here in two senses. First, the word indicates that the first-order short-period perturbations due to the second harmonic of the earth's gravitational potential have been computed analytically and then subtracted from the observations before the differential correction of the elements was performed. Second, the elements are mean in the sense that each set of them represents observations distributed along a two-day arc that represents approximately 25 revolutions of the satellite.

A quadratic polynomial in time was used to represent each of the elements except the inclination, for which we found that a linear expression was accurate enough. Then by a process of successive differential corrections we improved only the constant term of each polynomial to obtain a best least-squares fit of the orbit to the observations made during the two days, one before and one after the epoch of the elements. In the polynomial representing the mean anomaly we always corrected all three coefficients in order to take into account the rapid and unpredictable changes due to atmospheric drag.

As elements are determined for each day, the observations used in two successive determinations overlap for one day; we are thus assured of a better continuity in our results. The coefficients of the linear and quadratic terms of each polynomial were kept constant for periods of several weeks and were then readjusted.

The final results obtained for the mean elements are shown in Table I. The first column gives the Modified Julian Date (Julian Date minus 2,400,000.5) of the epoch of the elements. The succeeding columns give the argument of perigee (ω), the right ascension of the ascending node (Ω), the inclination (i), all expressed in degrees; the eccentricity (e); and the three coefficients M_o, M_1, and M_2 of the mean anomaly, expressed in revolutions, revolutions/day and revolutions/day^2, respectively. (It should be noticed that for M_o we give the accumulated values, but to avoid printing large figures we have systematically subtracted 12 revolutions every day.) The single digit placed at the right of each value represents the standard error and affects the last figure given. The next three columns contain the geocentric perigee distance (q) in megameters, the number of observations used (N) and the number of days (D) during which these observations were distributed. The number, σ , in the last column is a measure of the residuals of the observations. If the errors in all observations were equal to their respective (assumed) standard deviations, then σ would equal unity.

2. Description of Theoretical Orbit Computation

Our theoretical orbit computation is based on the well-known first-order differential equations relating the rate of change of the orbital elements to the perturbing accelerations (Moulton, 1914, Chapter X). We solve for the time dependence of the elements by first integrating these equations over an orbital period while keeping the elements constant during the integration. The integration can be carried out analytically for all perturbing accelerations except that due to air drag. The new values for the elements are then used to determine the changes in the elements during the next orbital period, and so forth. This iteration procedure is carried out on an IBM-7090 digital computer. The initial values used for the elements are those determined from the observations of the satellite. All future values are calculated by the iteration method. This method yields a very accurate estimate of the long period and secular contributions to the changes in the elements. However, the contributions of the short

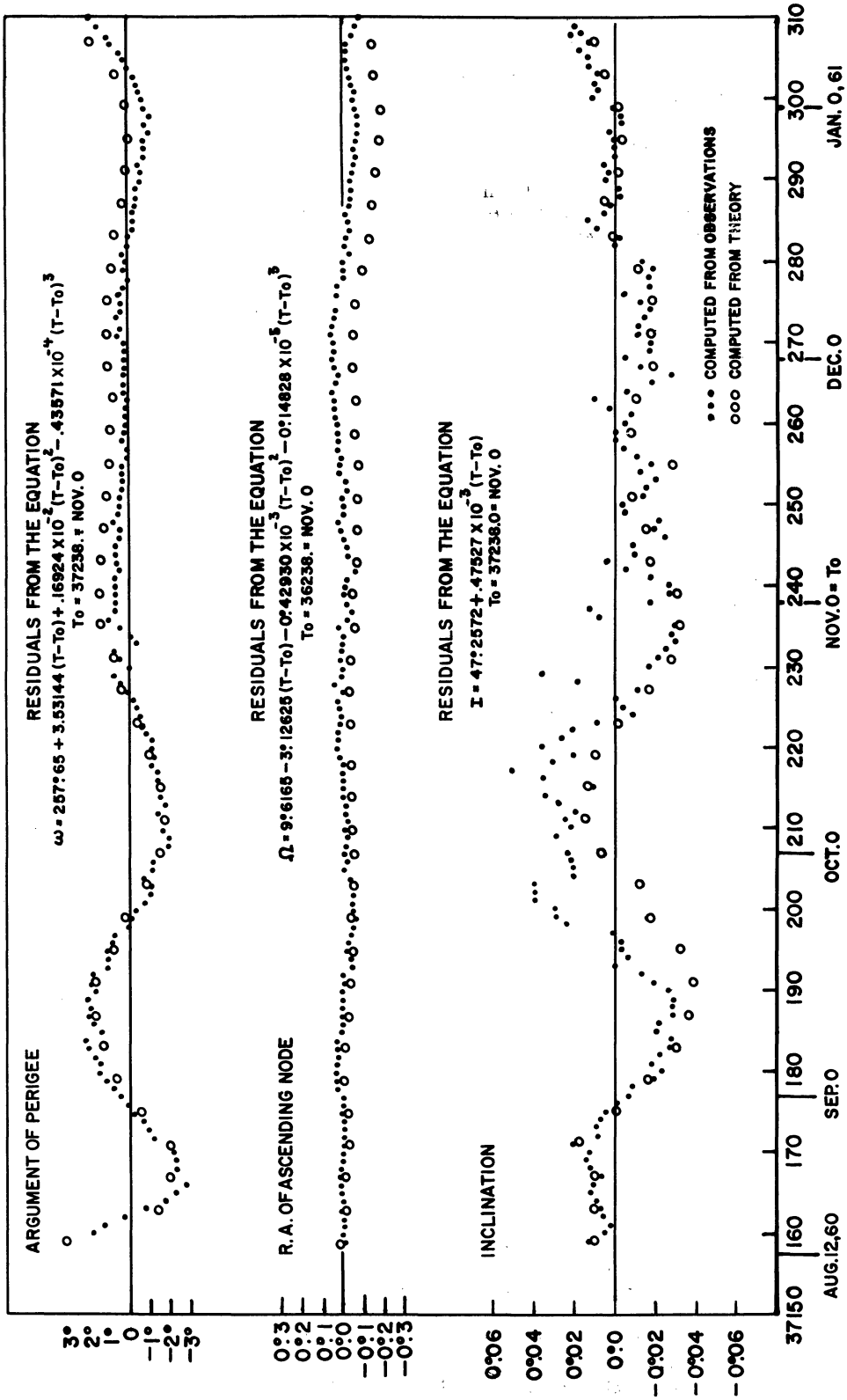

FIGURE 2.--Residuals of values of the argument of perigee, the right ascension of the ascending node, and the orbit of inclination with respect to polynomials obtained by least-squares fit.

period terms are averaged out.

At present, our computer program includes perturbations due to the following phenomena:

(1) Direct solar radiation pressure, including the effects of the earth's shadow.

(2) Neutral atmospheric drag (see Note 1). The atmospheric density is assumed to be spherically symmetric and constant in time, but this all-too-simple model is now being generalized.

(3) The second through the fifth harmonics of the earth's gravitational field.

(4) Solar and lunar gravitational fields.

(5) Solar radiation reflected from the earth (see Note 2). Our model for the reflection characteristics of the earth involves an arbitrary, but uniform, mixture of diffuse and specular reflection. However, only specular reflection is now included in our program.

It is clear that (aside from the approximate nature of our physical model and the errors accompanying observations) our theoretical and experimental elements differ even in principle. Our comparison below of the two sets of elements is based on the reasonable assumption that the differences that arise purely from the differing principles of element definition are very small and can be neglected in this analysis.

3. Comparison of Experimental and Theoretical Results

In calculating a theoretical orbit for Echo in order to compare it with results derived from the observations, we must consider the physical characteristics of the balloon. When launched, Echo was a sphere, 100 ± 1 ft in diameter, made of half-mil Mylar externally coated with an aluminum layer approximately $.2\mu$ thick. Its initial weight was 156.995 lb, including 33.34 lb of sublimating powders. The powders were of two kinds; the first (weighing 10 lb) was highly evaporative, while the second had a much lower vapor pressure.

The magnitude of the acceleration due to the pressure of sunlight is $K(A/M)(I/c)$, where (A/M) is the cross-sectional area-to-mass ratio of the satellite (initially 102 cm^2/gm); I is the solar energy flux; c is the velocity of light; and K is a scattering constant ($0 \leq K \leq 2$) whose value depends on the reflection characteristics of the surface. The constant c is known very accurately. For the solar constant we have used the value 2.00 cal/cm^2 min, with a probable error of 2 percent, quoted in the American Institute of Physics Handbook. The ratio A/M, on the other hand, is not known so accurately. Small holes that were introduced before launching and meteoric punctures will permit gas to escape at a rate almost impossible to predict. Hence, since 21 percent of the initial satellite mass was in the form of sublimating powders, it is difficult to determine purely theoretically the accurate time dependence of the satellite mass. The value of K is also uncertain: For specular reflection from a perfect sphere, $K = 1$; however, small irregularities in the shape or any diffuseness in the reflection of sunlight will tend to increase K. In view of these difficulties, we have considered $K(A/M)$ to be a (partially unknown) parameter and have allowed it to vary in a reasonable manner so as to obtain the best agreement between the theoretical and the observed variations in eccentricity.

In Figure 1, we have plotted the residuals of the eccentricity from a polynomial expression obtained by the method of least-squares. The experimentally deduced values are indicated by points, and the theoretical values by open circles. The rather close agreement between the two sets was obtained by assuming that $K = 1$ and that the total mass of the satellite decreased at the rate of .64 lb/day for the first 13 days, and then decreased at .16 lb/day. According to this model, only a small amount of the gas remained in the balloon on January 11, 1961. The decrease by a factor of four in the rate of mass loss, in spite of the expected increase in meteorite holes, may possibly be due to the escape of the more volatile of the two powders (see Note 3). These rates of mass loss are somewhat arbitrary; other rates may lead to equally good agreement with observations. However, the uncertainty in our value of $K(A/M)$ at any given time is probably not more than two or three percent. Further improvement in our estimate of $K(A/M)$ apparently will require consideration of other physical effects, such as a possible diurnal bulge of the atmosphere (see discussion below of the argument of perigee). Since we infer $K(A/M)$, as well

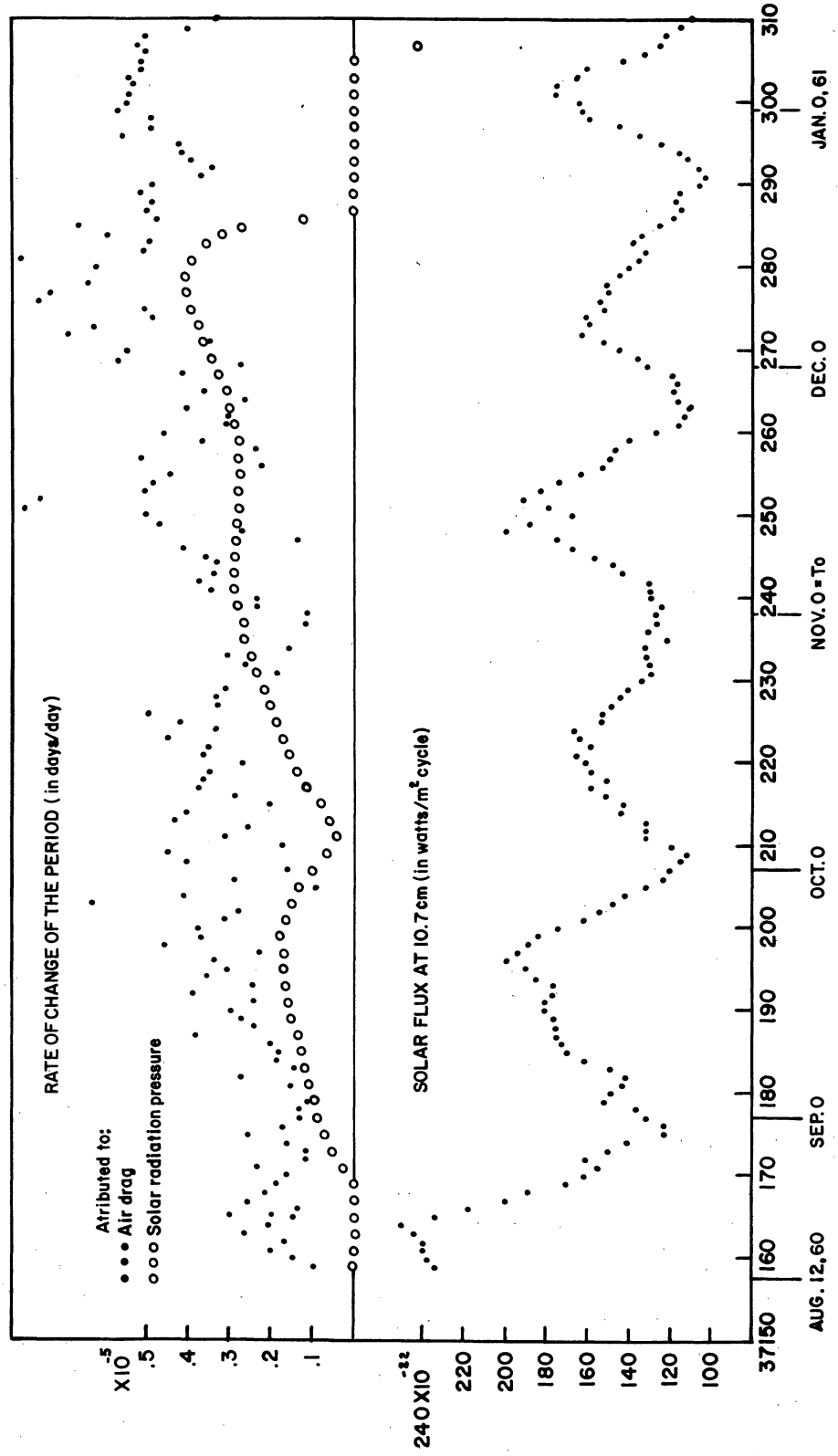

FIGURE 3. --Effects of solar activity on Echo I.

as an air density model, from the data, we may possibly be "covering up" small unexpected physical perturbations.

That the satellite did gradually lose a substantial portion of its mass (or that K increased gradually) can be seen from comparisons of the observed maximum value of the eccentricity ($e_{max} = .0788$) with the following theoretical calculations:

(1) By assuming that K(A/M) maintains its initial value of 102 cm^2/gm, we find $e_{max} = .0705$.

(2) By assuming that the satellite lost all of its gas soon after launching while K remained unity [$K(A/M) = 130\ cm^2/gm$], we obtain $e_{max} = .0885$.

We note that e reaches a maximum on or about December 27, 1960. Since we have plotted residuals from an equation with a positive slope, it is clear that the absolute values of these residuals will increase monotonically after that date.

We have also plotted in Figure 1 the residuals (from a polynomial) of the experimental and theoretical values of the geocentric perigee distance (q). The densities used in computing the theoretical curve were obtained by matching approximately a second-degree polynomial in altitude to ~~the logarithm~~ of the experimentally determined densities (see Section 4). The relatively high values of the theoretical perigee distance in the neighborhood of October 1, 1960, are due mainly to the correspondingly low values of the eccentricity. On the other hand, the relatively low theoretical values that persist after about November 1, 1960, are related to the "theoretical" air density values being somewhat greater than the average "observed" values. (This discrepancy could be largely eliminated by a small change in the density values used in the theoretical computation.)

Note that the perigee distance reaches its minimum value about two days later than the eccentricity reaches its maximum value. This is due to the decrease in semimajor axis caused by air drag. The explanation for the subsequent monotonic increase in both residuals is identical to that given in connection with the eccentricity variation.

In Figure 2, we have plotted the residuals (from polynomials) of the experimental and theoretical values of the argument of perigee (ω), the right ascension of the ascending node (Ω), and the orbital inclination (i).

We see that, for ω, the two curves are, in general, in good agreement until about November 1, 1960, at which time they start to deviate systematically. Part of the discrepancy -- about 15 percent -- would be eliminated by using an improved average air density. The remainder could be eliminated by reducing the rate of mass loss of the satellite, since the contribution to $\dot{\omega}$ due to radiation pressure is positive from 40 days after launch until January 11, 1961 (see Note 4). Of course, this change would introduce a significant disagreement in the eccentricity curves. Hence, these unexplained discrepancies must be due to minor deficiencies in our theoretical model and/or the accumulation of errors in numerical integration. To determine the likelihood of the latter possibility, we have carried out our numerical integration procedure beginning with the observationally deduced elements of November 2 and, again, from November 22, 1960. In both cases a significant discrepancy develops within a short time of the starting date. Since our theoretical computation gives such good results for the first 80 days, and since the calculations we have made on other satellites (e.g., 1958 Alpha and 1958 $\beta 2$) are in excellent agreement (within $\pm$ .2 deg) over much longer time periods, we feel that the discrepancy between theory and experiment is probably due to the inadequacy of our atmospheric model and our inadequate treatment of the sunlight scattered by the earth. In particular, the theoretical and experimental curves can be reconciled if we assume a bulge in the atmosphere (Jacchia, 1960). Such a bulge in the equi-density contours will be effective in changing ω when it intersects the orbit plane in a region asymmetrically placed with respect to the apsidal line. To estimate crudely the magnitude of this change in ω, consider the density to have a δ-function contribution superposed on the otherwise uniform density of the atmosphere along the satellite path. With the average, over-all density deduced from Table II, we find that ω can change at a maximum rate of .07 deg/day (see Note 5).

The theoretical and experimental residuals of Ω are in good agreement. The systematic deviations that do occur would be substantially eliminated by correcting the average densities. The residuals of the experimental and the theoretical values of i are in close agreement except for a short period near the end of September, 1960 (see Note 6).

In Figure 3 we have plotted the rate of change of period ($\dot{P}$) due to atmospheric drag and to solar radiation pressure: We computed first the total "observed" acceleration dP/dt; then, using the theory outlined in Section 2, we found the values of acceleration due to radiation pressure ($\dot{P}(R)$). These were then subtracted from dP/dt to obtain the accelerations $\dot{P}(D)$, which we attribute to air drag. We note that radiation pressure can have no effect on the period if the orbit is circular. However, if the orbit is noncircular and is partly in shadow, the satellite can enter and leave the shadow region at different distances from the sun, resulting in a net gain or loss of energy from the radiation field

As can be seen, the radiation pressure contribution to dP/dt is, in general, of the same order of magnitude as that of drag at these altitudes. Paradoxically, when perigee height is near its minimum value, the change in energy induced by radiation pressure is still comparable to that due to air drag, despite the increased air density. These facts can be understood in a qualitative way from the following argument: If the air density depends only on height, then as a function of eccentricity, the energy change due to air drag in one revolution is represented by a constant term plus terms in even powers of the eccentricity. On the other hand, when the qualifications given above are satisfied, the energy change per revolution due to radiation pressure is represented by a linear term plus higher powers in the eccentricity. Hence, the energy change due to radiation pressure can increase more rapidly with increasing eccentricity than can the energy change due to air drag when the atmospheric scale height is large. This provides a qualitative explanation of the results seen in Figure 3.

As may be seen from the end of the graph on Figure 3, the satellite lost energy to the solar radiation field until the end of December, 1960; then the satellite stayed in sunlight throughout its complete orbit for about two weeks. In January, 1961, the satellite began to gain energy from the solar radiation, in the manner described above. In fact, during the latter part of January, the satellite gained more energy from the solar radiation than was lost due to air drag. This marked the first time that an artificial satellite exhibited an actual increase in period.

4. Computation of Atmospheric Densities

It is generally assumed that the neutral air drag acceleration is given by

$$\frac{1}{2} C_D \left(\frac{A}{M}\right) v^2 \rho,$$

where C_D is a dimensionless aerodynamic drag coefficient; v is the velocity of the satellite relative to the atmosphere; and ρ is the atmospheric density. Using this assumption, one obtains a relations between $\dot{P}(D)$ and the air density ρ_p at the height of the perigee of the satellite's orbit. This relation is

$$\dot{P}(D) = -fC_D \left(\frac{A}{M}\right) \rho_p, \qquad (1)$$

where f is given by a rather complicated function of the orbital eccentricity, the oblateness of the earth, and the (assumed) velocity of rotation of the atmosphere (Sterne, 1959). In the derivation of this formula

it was assumed that the atmospheric density at an altitude ΔZ above perigee can be expressed by

$$\rho = \rho_P \exp\left(-\frac{\Delta Z}{H}\right),$$

where H is the scale height.

There are several difficulties associated with inferring atmospheric densities from equation (1). First, it is neccessary to use the appropriate $\dot{P}$. With the mean anomaly represented by a polynomial like $M = M_o + M_1 (t - t_o) + M_2 (t - t_o)^2$, where t_o is the epoch of the elements, it is usual to consider the rate of change of the period given by $\dot{P} = -2M_2/M_1^2$. This form, however, leads to a difficulty because the mean anomaly is measured from perigee, the angular motion of which is subject to relatively large variations due to the solar radiation pressure. On the other hand, equation (1) was derived on the assumption that the perigee position is stationary. Therefore, in order to use an equivalent $\dot{P}$, we corrected M_2 for the contribution due to the mean acceleration of ω. We then calculated $\dot{P}(D)$ by subtracting $\dot{P}(R)$ from the "corrected" values of $\dot{P}$.

Second, it is not clear what value should be used for C_D. The concepts usually employed in calculating C_D, such as a definite temperature and a single mean free path of the air molecules, may require considerable modifications for the high altitudes traversed by Echo. If, however, a future analysis indicates that a different (but constant) value of C_D should be used, then it will be quite simple to correct our density determinations.

Third, it is difficult to determine a meaningful value for the scale height since densities at different altitudes have been calculated for different periods of time. Since the density at each altitude suffers large fluctuations in time, comparing densities at different altitudes at different times is inadequate for determining the relation between densities at different altitudes at the same time. For example, we note (see Table II) that averaging over the fluctuations yields an almost constant value of the density between the altitudes 950 km and 1200 km. This unusual result is probably due to perigee having passed through the 950 km region during a minimum of the 10.7cm solar flux variations.

In our computation we assumed that the ratio (A/M) varies with time (as determined from our theoretical match with the experimental variations in eccentricity), and that C_D has the value 2.5 (Stirton, 1960). Air densities corresponding to the two tentative scale height values of 200 and 400 km were then computed. Our results are given in Table II. In the first column we give the Modified Julian Day defined above; and in the second column, the height of perigee in kilometers above the International Ellipsoid. In the next two columns, we give the rates of change of the period attributed to air drag $[\dot{P}(D)]$ and to solar radiation pressure $[\dot{P}(R)]$, respectively. Finally, in the last two columns we give the decimal logarithms of atmospheric densities corresponding to H = 0.200 megameter and H = 0.400 megameter. (We did not plot these values because their variations follow very closely the pattern of the $\dot{P}(D)$ curve given in Figure 3.)

Due to all the uncertainties affecting the parameters involved in our computations, the densities we have inferred from the orbit of Echo I must be considered as provisional.

5. Lifetime of Echo

Because of our imprecise knowledge of air densities it is very difficult to predict the lifetime of Echo I. We do know, however, that the perigee altitude (and eccentricity) oscillate with a peak-to-peak period of about 300 days (see Note 7). In fact, as can be seen from Figure 1, the day perigee altitude reached its minimum value is in exact accord with our theoretical calculation.

In view of the large amplitude oscillation of perigee height, it is most likely that the satellite will perish on one of these regular dips of perigee into the atmosphere. Hence, one can estimate the month of "death" as accurately as the year. To the best of our knowledge, the balloon will stop orbiting during its fourth dip in July, 1963, if its shape is not substantially changed before then. In view of the decrease in air density to be expected in the next few years, in accordance with the correlation between sunspot activity and upper atmosphere densities (see Note 8), the balloon may survive until 1964.

Notes

1. Charge drag is quite small for the Echo satellite and has been ignored.

2. The infrared radiation from the earth, if it were uniform, would only have the effect of changing the earth's mass by an entirely negligible amount, provided that the satellite always presented the same cross-sectional area towards the earth. (This last requirement is clearly satisfied for the case of the spherical Echo.) Preliminary investigations of the infrared radiation from the earth (Intermountain Weather, Inc., Final Report under Contract AF 19 (604) -2418) indicate that at 1000 km this radiation is with in $\pm$ 10 percent of uniformity. Since the re-radiated power at 1000 km is only a small fraction of that of direct radiation, the effect of the former on the orbit is probably quite small.

3. The slow final rate of mass loss could not be measurably influenced by any accumulation of air molecules penetrating only one surface of the balloon, since it is possible to show that the balloon has collided so far with less than one pound of air.

4. Except for the first week after launch, $\dot{\omega}$ due to radiation pressure is negligibly small until early October, 1960. However, we note that sunlight pressure contributes 15 percent to the 3.5 deg/day mean rate of change of ω.

5. This example is intended to show only that the magnitude of the discrepancy can be explained by an atmospheric bulge consistent with the average density; it is not meant to be taken as a literal explanation for the discrepancy. For example, at these altitudes, it is possible that bulges occur only after severe solar flares.

6. The change in i due to a rigid rotation of the atmosphere was not included in our theoretical computations. Its cumulative value on January 11, 1961, would be about -.006 deg.

7. More accurately, the period from maximum-to-maximum value of perigee altitude is 307 days, while the minimum-to-minimum period varies.

8. For this and other useful suggestions, we thank Dr. L. G. Jacchia.

References

JACCHIA, L. G.
1960. A variable atmospheric-density model from satellite accelerations. Journ. Geophys. Res., vol. 65, pp. 2775-2782

MOULTON, F. R.
1914. An introduction to celestial mechanics. Macmillan Co., New York.

PARKINSON, R. W., JONES, H. M., and SHAPIRO, I. I.
1960. Effects of solar radiation pressure on earth satellite orbits. Science vol. 131, pp. 920-921

SHAPIRO, I. I., and JONES, H. M.
1960. Perturbations of the orbit of the Echo balloon. Science, vol. 132, pp. 1484-1486.

STERNE, T. E.
1959. Effect of the rotation of a planetary atmosphere upon the orbit of a close satellite. Journ. Amer. Rocket Soc., vol. 29, pp 777-782.

STIRTON, R. J.
1960. The upper atmosphere and satellite drag. Smithsonian Contr. Astrophys., vol. 5, pp. 9-15.

ZADUNAISKY, P. E.
1960. The orbit of Satellite 1958 α1 (Explorer I) during the first 10500 revolutions. Smithsonian Astrophys. Obs., Spec. Rep. No. 50, 28 pp.

TABLE I

ORBITAL ELEMENTS OF THE SATELLITE 1960 IOTA ONE

AUGUST, 1960

MJD	ω	Ω	i	e	M_o	M_1	M_2	q	N	D	σ
37159.0	14.0 1	254.644 3	47.232 2	.01029 2	.5309 4	12.17731 2	-.18E-3 3	7.898038	88	2	.61
37160.0	14.9 1	251.556 3	47.226 2	.01069 3	.7087 3	12.177039 6	-.14E-3 1	7.894933	77	2	.69
37161.0	16.9 1	248.455 3	47.224 2	.01089 2	.8840 3	12.176802 7	-.10E-3 1	7.893462	/42	2	.79
37162.0	18.5 1	245.375 2	47.228 1	.01123 2	1.0606 3	12.176562 5	-.123E-3 8	7.890857	/69	2	.76
37163.0	19.9 1	242.298 3	47.230 1	.01162 3	1.2378 3	12.176362 6	-.54E-3 1	7.887850	94	2	.59
37164.0	21.5 1	239.210 3	47.232 2	.01211 3	1.4148 3	12.176219 7	-.10E-3 1	7.883938	80	2	.70
37165.0	23.51 8	236.132 2	47.235 1	.01261 3	1.5911 2	12.176005 7	-.14E-3 1	7.880103	/49	2	.61
37166.0	25.6 1	233.047 2	47.235 1	.01306 4	1.7674 3	12.175715 1	-.15E-3 4	7.876634	98	2	.50
37167.0	29.0 2	229.946 6	47.231 3	.01348 8	1.9407 5	12.175672 3	-.6E-4 2	7.873272	39	2	.89
37168.0	31.4 1	226.867 3	47.237 1	.01392 5	2.1166 3	12.175454 8	-.9E-4 1	7.869878	75	2	.58
37169.0	34.06 8	223.770 3	47.240 2	.01443 4	2.2925 2	12.175244 7	-.12E-3 1	7.865889	65	2	.49
37170.0	36.87 8	220.678 3	47.238 3	.01490 4	2.4681 2	12.174993 7	-.13E-3 1	7.862241	51	2	.54
37171.0	39.81 7	217.585 2	47.246 1	.01538 4	2.6436 2	12.17500 1	+.21E-3 1	7.858420	/59	2	.53
37172.0	43.39 3	214.498 2	47.235 1	.01615 4	2.8176 8	12.17532 1	.13E-3 1	7.852091	/08	2	1.70
37173.0	46.33 4	211.404 3	47.236 1	.01663 4	2.9937 1	12.17562 1	.14E-3 1	7.848156	/12	2	1.32
37174.0	49.43 7	208.340 4	47.2351 8	.01725 3	3.1695 2	12.17594 1	.18E-3 1	7.843055	/20	2	1.04
37175.0	52.53 3	205.242 2	47.2321 7	.01799 3	3.34576 9	12.176373 7	.255E-3 9	7.836952	/24	2	.94
37176.0	55.69 3	202.154 2	47.227 1	.01860 2	3.52232 8	12.176860 5	.20E-3 1	7.831907	82	2	.80
37177.0	58.91 5	199.062 3	47.2217 9	.01910 1	3.6991 1	12.177277 7	.175E-3 8	7.827737	63	2	.80

TABLE 1 (cont.)

ORBITAL ELEMENTS OF THE SATELLITE 1960 IOTA ONE

SEPTEMBER, 1960

MJD	ω	Ω	i	e	M_o	M_1	M_2	q	N	D	σ
37178.0	62.07 6	196.001 4	47.2206 8	.01965 3	3.8764 2	12.17763 1	.18E-3 1	7.823203	99	2	.80
37179.0	65.32 8	192.913 4	47.211 1	.02029 5	4.0538 2	12.17798 1	.18E-3 2	7.817934	144	2	1.11
37180.0	68.50 5	189.813 3	47.207 1	.02092 5	4.2318 2	12.17837 2	.16E-3 2	7.812761	104	2	1.17
37181.0	71.42 7	186.725 3	47.214 2	.02160 4	4.4108 2	12.17873 1	.21E-3 2	7.807172	62	2	.85
37182.0	74.69 5	183.620 3	47.208 1	.02228 5	4.5892 1	12.17923 1	.30E-3 3	7.801502	78	2	.94
37183.0	77.83 3	180.531 2	47.205 1	.02297 4	4.76857 9	12.179800 9	.21E-3 3	7.795746	59	2	1.12
37184.0	80.90 6	177.446 4	47.204 2	.02363 6	4.9486 2	12.18024 2	.24E-3 3	7.790326	33	2	2.01
37185.0	83.2 2	174.326 9	47.212 4	.02450 7	5.1310 6	12.18071 2	.23E-3 2	7.783167	54	2	1.72
37186.0	86.5 1	171.222 4	47.211 2	.02515 4	5.3114 3	12.18126 1	.26E-3 1	7.777730	94	2	1.14
37187.0	89.69 7	168.129 5	47.205 2	.02573 5	5.4925 2	12.18178 1	.41E-3 3	7.772899	109	2	1.00
37188.0	92.78 8	165.035 6	47.205 2	.02622 6	5.6746 2	12.18260 2	.14E-3 4	7.768661	94	2	1.18
37189.0	95.88 2	161.952 2	47.2056 9	.02689 4	5.85708 6	12.183064 8	.33E-3 2	7.763138	85	2	1.23
37190.0	98.58 9	158.848 9	47.208 5	.02762 8	6.0413 2	12.18375 2	.35E-3 2	7.756950	52	2	1.11
37191.0	101.8 1	155.74 2	47.216 9	.02827 6	6.2250 3	12.18437 2	.31E-3 2	7.751529	34	2	1.20
37192.0	104.8 2	152.66 2	47.20 2	.0289 1	6.4096 5	12.18514 2	.42E-3 5	7.746067	25	2	1.54
37193.0	107.2 2	149.51 1	47.236 7	.02948 5	6.5967 4	12.18578 3	.32E-3 2	7.741288	31	2	2.08
37194.0	110.35 8	146.419 8	47.230 4	.03019 3	6.7824 2	12.18652 1	.41E-3 2	7.735319	36	2	1.18
37195.0	113.47 5	143.347 2	47.234 2	.03074 2	6.9689 1	12.187448 8	.32E-3 1	7.730541	30	2	.97
37196.0	116.49 6	140.245 8	47.234 7	.03149 6	7.1564 2	12.188112 2	.35E-3 1	7.724259	24	2	.89
37197.0	119.49 6	137.131 7	47.240 7	.03220 5	7.3446 1	12.18877 2	.26E-3 3	7.718306	23	2	.81
37198.0	121.92 5	134.021 7	47.263 6	.03262 4	7.5351 2	12.18930 2	.44E-3 3	7.714769	43	2	.81
37199.0	124.90 5	130.914 6	47.269 5	.03318 3	7.7248 1	12.190068 9	.37E-3 2	7.710000	55	2	.73
37200.0	127.97 6	127.827 3	47.270 7	.03389 4	7.9150 2	12.190682 8	.37E-3 2	7.704076	38	2	.71
37201.0	130.79 9	124.723 4	47.29 1	.03450 6	8.1066 2	12.19134 2	.32E-3 2	7.698915	31	2	1.32
37202.0	133.7 1	121.624 5	47.29 1	.03505 8	8.2986 3	12.19201 3	.29E-3 4	7.694244	29	2	1.58
37203.0	136.8 2	118.50 2	47.29 1	.0356 1	8.4907 4	12.19261 3	.56E-3 7	7.689423	25	2	2.25
37204.0	140.51 6	115.439 8	47.267 5	.03601 6	8.6819 2	12.19310 2	.4E-4 4	7.686119	29	2	1.03
37205.0	143.40 3	112.357 5	47.267 3	.03671 4	8.8759 1	12.19354 1	.13E-3 2	7.680385	37	2	.77
37206.0	146.61 5	109.246 7	47.265 4	.03723 5	9.0695 1	12.194820 8	.32E-3 2	7.675675	37	2	1.17
37207.0	149.70 3	106.155 1	47.267 1	.03775 3	9.26399 8	12.19536 1	.21E-3 2	7.671291	38	2	.86

TABLE I (cont.)

ORBITAL ELEMENTS OF THE SATELLITE 1960 IOTA ONE

OCTOBER, 1960

MJD	ω	Ω	i	e	M_o	M_1	M_2	q	N	D	σ
37208.0	152.52 3	103.048 1	47.263 1	.03828 3	9.45972 6	12.19582 1	.31E-3 3	7.666878	37	2	.84
37209.0	155.82 6	99.942 3	47.274 2	.03877 5	9.6547 2	12.19541 3	.34E-3 5	7.663189	40	2	2.13
37210.0	159.33 8	96.824 6	47.266 5	.03927 4	9.8495 2	12.19568 2	.12E-3 4	7.659021	27	2	1.09
37211.0	162.68 5	93.726 4	47.271 4	.03968 3	10.0452 1	12.19592 1	.22E-3 3	7.655668	33	2	.84
37212.0	166.36 6	90.612 4	47.265 4	.04023 5	10.2404 2	12.19630 2	.18E-3 3	7.651119	25	2	1.14
37213.0	169.36 4	87.515 1	47.275 1	.04067 5	10.4379 1	12.19665 2	.32E-3 4	7.647510	22	2	1.44
37214.0	172.89 4	84.406 2	47.282 2	.04110 3	10.6345 1	12.197279 7	.30E-3 1	7.643776	30	2	.96
37215.0	176.33 5	81.306 2	47.258 5	.04152 4	10.8321 1	12.19777 2	.17E-3 4	7.640282	24	2	.60
37216.0	179.77 6	78.198 3	47.284 6	.04179 5	11.0302 2	12.19822 1	.23E-3 3	7.637930	21	2	.86
37217.0	183.23 7	75.096 4	47.30 1	.04211 9	11.2288 2	12.19868 1	.32E-3 4	7.635127	23	2	1.37
37218.0	186.93 9	71.986 4	47.28 1	.04258 9	11.4274 3	12.19925 2	.32E-3 5	7.631193	26	2	1.39
37219.0	190.31 7	68.871 5	47.27 1	.04282 7	11.6275 2	12.19975 2	.32E-3 5	7.629019	27	2	1.32
37220.0	193.78 8	65.777 6	47.286 9	.04321 7	11.8280 2	12.20029 2	.26E-3 4	7.625724	28	2	1.22
37221.0	197.26 5	62.674 7	47.277 5	.04354 3	12.0292 2	12.20098 1	.34E-3 3	7.622776	45	2	1.34
37222.0	200.96 4	59.563 5	47.272 4	.04396 3	12.2305 1	12.20161 1	.34E-3 2	7.619200	49	2	1.01
37223.0	204.61 4	56.437 4	47.260 4	.04432 2	12.4328 1	12.20238 9	.42E-3 2	7.616039	48	2	.72
37224.0	208.14 4	53.314 4	47.242 4	.04488 2	12.6363 1	12.20304 8	.34E-3 2	7.611307	66	2	.80
37225.0	211.79 3	50.206 5	47.248 2	.04532 2	12.84015 9	12.203777 7	.41E-3 2	7.607424	84	2	.68
37226.0	215.40 3	47.101 6	47.252 2	.04569 2	13.04503 9	12.20460 1	.46E-3 3	7.604174	55	2	.61
37227.0	219.1 1	43.96 1	47.241 7	.04624 6	13.2505 4	12.20518 3	.35E-3 5	7.599512	26	2	2.07
37228.0	223.0 1	40.88 1	47.272 7	.04684 5	13.4560 4	12.20584 1	.36E-3 2	7.594515	29	2	.83
37229.0	226.9 2	37.81 2	47.29 1	.04722 6	13.6623 6	12.20657 2	.35E-3 2	7.591145	24	2	.88
37230.0	229.62 1	34.602 6	47.236 3	.04763 3	13.8734 2	12.20714 5	.289E-3 6	7.587644	58	4	.80
37231.0	233.52 6	31.498 8	47.233 2	.04789 4	13.9812 2	12.20773 3	.27E-3 5	7.585302	35	2	.67
37232.0	237.3 1	28.372 9	47.229 2	.04818 4	14.2902 3	12.208375 9	.34E-3 2	7.582720	48	2	.52
37233.0	239.61 4	25.245 7	47.225 1	.04890 3	14.5044 1	12.209138 4	.368E-3 6	7.576742	83	4	1.16
37234.0	243.62 7	22.12 1	47.228 3	.04919 5	14.7143 2	12.20994 4	.26E-3 6	7.574076	35	2	1.49
37235.0	247.45 8	19.02 1	47.226 3	.04978 6	14.9253 2	12.21050 8	.78E-3 8	7.569163	29	2	1.39
37236.0	251.61 9	15.84 1	47.265 8	.0509 1	15.1368 3	12.21141 5	.45E-3 5	7.559672	13	2	1.10
37237.0	254.8 2	12.70 3	47.27 2	.0515 2	15.3516 5	12.21220 3	.23E-3 3	7.554702	30	4	3.37
37238.0	258.4 2	9.60 2	47.24 2	.0513 2	15.5660 5	12.21260 4	.25E-3 2	7.556376	30	4	2.65

TABLE I (cont.)

ORBITAL ELEMENTS OF THE SATELLITE 1960 IOTA ONE

NOVEMBER, 1960

MJD	ω	Ω	i	e	M_o	M_1	M_2	q	N	D	σ
37239.0	261.92 5	6.483 5	47.231 4	.05218 6	15.7815 2	12.21578 1	.40E-3 2	7.547844	24	2	1.13
37240.0	265.44 2	3.361 2	47.232 2	.05265 2	15.99768 5	12.216571 5	.39E-3 1	7.543801	49	2	.66
37241.0	268.94 2	.223 2	47.241 2	.05308 2	16.2148 5	12.217462 7	.48E-3 2	7.539995	63	2	.59
37242.0	272.33 5	-2.96 1	47.254 4	.05370 4	16.4332 1	12.21834 2	.50E-3 4	7.534714	36	2	.81
37243.0	275.99 3	-6.067 6	47.264 3	.05427 3	16.65163 9	12.219276 4	.478E-3 4	7.529722	83	4	.85
37244.0	279.54 2	-9.173 4	47.251 2	.05489 2	16.87131 7	12.220232 4	.471E-3 3	7.524467	87	4	.67
37245.0	283.07 3	-12.305 5	47.252 2	.05538 3	17.09201 9	12.221184 8	.49E-3 1	7.520144	62	2	.68
37246.0	286.48 3	-15.418 5	47.237 3	.05588 3	17.31390 9	12.22213 1	.53E-3 2	7.515808	42	2	.60
37247.0	290.00 6	-18.538 5	47.242 3	.05641 3	17.5365 2	12.23311 2	.32E-3 4	7.511117	23	2	.59
37248.0	293.89 7	-21.66 1	47.241 5	.05706 5	17.7590 2	12.22404 2	.42E-3 3	7.505586	43	2	1.03
37249.0	297.17 5	-24.823 7	47.258 4	.05752 4	17.9843 2	12.22514 1	.57E-3 2	7.501487	55	2	1.03
37250.0	300.65 3	-27.959 1	47.259 1	.05811 2	18.21013 9	12.226294 4	.594E-3 3	7.496311	86	4	1.11
37251.0	304.21 4	-31.088 5	47.250 3	.05866 3	18.4368 1	12.22767 2	.91E-3 3	7.491363	29	2	.53
37252.0	307.59 7	-34.257 8	47.248 7	.05874 6	18.6659 2	12.22967 4	.85E-3 6	7.489901	49	2	1.77
37253.0	311.14 6	-37.387 6	47.245 5	.05928 5	18.8960 2	12.23061 2	.25E-3 3	7.485249	55	2	1.59
37254.0	314.76 1	-40.501 1	47.252 2	.06009 1	19.12662 5	12.231728 5	.578E-3 8	7.478333	61	2	1.70
37255.0	318.27 3	-43.642 2	47.248 2	.06065 2	19.35890 7	12.232850 7	.54E-3 1	7.473423	68	2	1.79
37256.0	321.52 7	-46.792 4	47.255 4	.06059 6	19.5931 2	12.23388 2	.40E-3 3	7.473483	62	2	1.55
37257.0	325.19 5	-49.914 5	47.262 4	.06128 5	19.8268 2	12.23479 1	.61E-3 2	7.467659	70	2	1.21
37258.0	328.90 1	-53.065 1	47.267 2	.06199 2	20.06142 4	12.235680 5	.391E-3 9	7.461622	91	2	.74
37259.0	332.35 2	-56.206 1	47.268 1	.06239 2	20.29766 5	12.236644 4	.494E-3 8	7.458014	99	2	.65
37260.0	335.88 3	-59.350 3	47.263 3	.06289 3	20.53471 9	12.23774 1	.57E-3 2	7.453657	61	2	.87
37261.0	339.39 5	-62.492 2	47.260 4	.06334 4	20.7729 1	12.23879 1	.45E-3 3	7.449581	50	2	.95
37262.0	342.79 5	-65.636 3	47.272 4	.06377 4	21.0124 2	12.239687 9	.45E-3 2	7.445802	44	2	.84
37263.0	346.37 9	-68.78 1	47.28 1	.06415 8	21.2523 2	12.24069 2	.53E-3 3	7.442441	21	2	1.11
37264.0	350.07 6	-71.919 8	47.264 5	.06466 6	21.4929 2	12.24173 3	.44E-3 5	7.437927	24	2	.55
37265.0	353.64 5	-75.096 8	47.252 4	.06512 6	21.7349 2	12.24272 2	.51E-3 3	7.433880	36	2	.71
37266.0	357.16 4	-78.263 9	47.243 4	.06565 5	21.9780 1	12.24373 1	.50E-3 2	7.429214	50	2	.78
37267.0	360.62 4	-81.388 4	47.259 3	.06606 4	22.2223 1	12.24478 1	.56E-3 2	7.425528	51	2	.90
37268.0	364.13 4	-84.540 9	47.267 3	.06649 5	22.4675 1	12.24585 1	.47E-3 3	7.421735	31	2	.81

TABLE I (cont.)

ORBITAL ELEMENTS OF THE SATELLITE 1960 IOTA ONE

DECEMBER, 1960

MJD	ω	Ω	i	e	M_o	M_1	M_2	q	N	D	σ
37269.0	367.65 4	-87.708 9	47.254 3	.06708 6	22.7137 1	12.24703 2	.69E-3 4	7.416509	39	2	1.03
37270.0	371.17 5	-90.86 1	47.255 3	.06764 8	22.9613 1	12.24848 3	.68E-3 4	7.411485	29	2	1.14
37271.0	374.99 8	-94.01 1	47.262 4	.0685 1	23.2094 2	12.24989 6	.55E-3 6	7.403919	27	2	1.43
37272.0	378.4 1	-97.17 2	47.262 4	.0691 1	23.4599 2	12.25124 6	.8E-3 1	7.398853	26	2	1.51
37273.0	381.96 4	-100.345 5	47.258 3	.06937 5	23.7118 1	12.252742 5	.76E-3 1	7.396072	56	4	1.65
37274.0	385.31 4	-103.512 8	47.257 2	.06963 5	23.9656 1	12.25441 4	.66E-3 4	7.393305	27	2	.81
37275.0	388.72 6	-106.62 1	47.263 3	.07021 8	24.2207 2	12.25587 2	.69E-3 6	7.388099	60	2	1.58
37276.0	392.35 3	-109.843 5	47.271 3	.07078 9	24.4769 1	12.25772 2	.89E-3 6	7.382792	77	2	1.86
37277.0	395.61 5	-113.013 9	47.259 3	.07123 8	24.7360 1	12.25935 4	.86E-3 5	7.378601	39	2	1.13
37278.0	398.8 2	-116.21 3	47.26 2	.0715 5	24.9969 7	12.2611 1	.8E-3 2	7.375950	12	2	2.60
37279.0	402.54 7	-119.38 1	47.257 5	.0724 1	25.2579 2	12.26260 3	.63E-3 6	7.368322	18	2	1.05
37280.0	405.87 5	-122.547 5	47.264 3	.07289 9	25.5215 2	12.26399 2	.79E-3 8	7.363573	19	2	.96
37281.0	409.5 1	-125.75 2	47.23 1	.0740 3	25.7856 4	12.26560 7	.9E-3 3	7.354034	17	2	2.68
37282.0	412.58 3	-128.902 4	47.278 2	.07391 5	26.05306 9	12.26698 3	.67E-3 4	7.354226	33	2	.77
37283.0	415.94 3	-132.071 4	47.278 2	.07451 5	26.32089 9	12.26838 1	.72E-3 3	7.348955	40	2	.84
37284.0	419.15 2	-135.270 2	47.289 2	.07491 5	26.59068 6	12.26989 2	.78E-3 3	7.345138	38	2	1.50
37285.0	422.56 3	-138.437 1	47.294 2	.07567 6	26.8613 1	12.271373 7	.70E-3 1	7.338527	37	2	1.14
37286.0	425.89 3	-141.611 2	47.285 1	.07610 6	27.13350 8	12.272360 5	.46E-3 1	7.334717	38	2	1.04
37287.0	429.24 2	-144.804 3	47.284 1	.07656 7	27.40654 6	12.273181 6	.38E-3 1	7.330772	43	2	1.98
37288.0	432.53 2	-147.994 3	47.279 3	.07697 4	27.68051 7	12.273946 9	.38E-3 2	7.327222	32	2	.61
37289.0	435.84 2	-151.176 1	47.280 3	.07739 4	27.95516 5	12.274694 5	.393E-3 9	7.323543	36	2	.69
37290.0	439.13 2	-154.351 1	47.287 2	.07766 6	28.23061 7	12.27604 1	.35E-3 1	7.320841	37	2	1.72
37291.0	442.41 1	-157.545 1	47.287 2	.07805 2	28.5069 4	12.27667 2	.26E-3 4	7.317529	34	2	2.22
37292.0	445.77 2	-160.734 2	47.288 2	.07826 1	28.7835 1	12.27727 2	.24E-3 6	7.315663	22	2	1.42
37293.0	448.95 5	-163.930 3	47.284 2	.07845 2	29.0613 1	12.277847 3	.285E-3 4	7.313856	34	4	2.43
37294.0	452.26 4	-167.115 2	47.284 1	.07873 2	29.3393 1	12.278460 3	.298E-3 4	7.311441	30	4	1.34
37295.0	455.6 2	-170.309 6	47.285 3	.07880 6	29.6178 5	12.27907 3	.30E-3 1	7.310643	25	4	4.19
37296.0	458.6 1	-173.509 6	47.288 3	.07880 5	29.8981 4	12.279876 6	.408E-3 7	7.310327	35	4	4.28
37297.0	462.02 5	-176.697 7	47.282 6	.07874 5	30.1782 2	12.28063 1	.35E-3 2	7.310455	27	4	1.33
37298.0	465.21 8	-179.90 2	47.283 7	.07873 5	30.4596 3	12.28137 3	.35E-3 2	7.310259	20	4	1.27
37299.0	468.68 4	-183.074 6	47.288 3	.07864 3	30.7408 1	12.282158 6	.415E-3 8	7.310673	30	4	.84

TABLE I (cont.)

ORBITAL ELEMENTS OF THE SATELLITE 1960 IOTA ONE
JANUARY, 1961

MJD	ω	Ω	i	e	M_o	M_1	M_2	q	N	D	σ
37300.0	472.00 3	-186.270 5	47.297 3	.07843 4	31.02349 9	12.282965 6	.401E-3 4	7.312036	26	4	.63
37301.0	475.34 3	-189.461 4	47.297 3	.07822 3	31.30689 9	12.283759 6	.397E-3 5	7.313328	27	4	.62
37302.0	478.75 2	-192.655 3	47.298 4	.07797 4	31.59090 7	12.284547 6	.389E-3 5	7.315065	45	4	.64
37303.0	482.15 2	-195.843 3	47.297 2	.07763 4	31.87572 7	12.285327 5	.395E-3 4	7.317390	56	4	.56
37304.0	485.58 2	-199.028 2	47.302 1	.07732 3	32.16131 5	12.286105 4	.378E-3 3	7.319552	76	4	.57
37305.0	488.99 2	-202.219 2	47.303 1	.07689 3	32.44772 5	12.286869 3	.376E-3 2	7.322711	86	4	.60
37306.0	492.36 2	-205.4117 1	47.3079 8	.07648 3	32.73509 6	12.287563 3	.333E-3 4	7.325638	91	4	.73
37307.0	495.85 3	-208.611 3	47.303 2	.07610 3	33.02282 8	12.288163 5	.269E-3 5	7.328435	83	4	.71
37308.0	499.24 3	-211.796 3	47.298 2	.07571 4	33.3114 1	12.288628 4	.223E-3 4	7.331334	77	4	.84
37309.0	502.69 3	-214.985 5	47.301 3	.07529 5	33.60027 9	12.288991 6	.127E-3 5	7.334491	75	4	1.24
37310.0	506.25 3	-218.183 1	47.2949 9	.07519 4	33.88922 9	12.289201 5	.064E-3 3	7.335265	87	4	.91

TABLE II

ATMOSPHERIC DENSITIES COMPUTED FROM THE MOTION OF SATELLITE ECHO I

MJD	Z	$\dot{P}$(D)	$\dot{P}$(R)	LOG RHO H=0.200	LOG RHO H=0.400
37159.	1520.	-0.927E-06	-0.168E-07	-18.099	-18.179
37160.	1517.	-0.149E-05	0.114E-07	-17.888	-17.971
37161.	1516.	-0.203E-05	0.311E-08	-17.756	-17.839
37162.	1514.	-0.174E-05	0.332E-08	-17.819	-17.904
37163.	1511.	-0.270E-05	0.584E-08	-17.626	-17.712
37164.	1507.	-0.204E-05	0.162E-07	-17.744	-17.833
37165.	1504.	-0.150E-05	0.196E-07	-17.873	-17.964
37166.	1500.	-0.137E-05	0.235E-07	-17.909	-18.003
37167.	1498.	-0.258E-05	0.214E-07	-17.632	-17.727
37168.	1495.	-0.218E-05	0.192E-07	-17.703	-17.800
37169.	1491.	-0.191E-05	0.230E-07	-17.755	-17.854
37170.	1488.	-0.163E-05	0.181E-07	-17.819	-17.919
37171.	1485.	-0.238E-05	-0.312E-06	-17.651	-17.753
37172.	1479.	-0.118E-05	-0.436E-06	-17.949	-18.054
37173.	1476.	-0.119E-05	-0.561E-06	-17.942	-18.049
37174.	1471.	-0.164E-05	-0.650E-06	-17.798	-17.907
37175.	1466.	-0.259E-05	-0.710E-06	-17.594	-17.705
37176.	1461.	-0.175E-05	-0.808E-06	-17.759	-17.872
37177.	1458.	-0.132E-05	-0.890E-06	-17.878	-17.993
37178.	1454.	-0.133E-05	-0.963E-06	-17.872	-17.988
37179.	1449.	-0.113E-05	-0.102E-05	-17.936	-18.054
37180.	1444.	-0.940E-06	-0.108E-05	-18.012	-18.132
37181.	1439.	-0.156E-05	-0.113E-05	-17.786	-17.908
37182.	1434.	-0.272E-05	-0.118E-05	-17.539	-17.663
37183.	1428.	-0.147E-05	-0.123E-05	-17.804	-17.929
37184.	1423.	-0.182E-05	-0.128E-05	-17.705	-17.832
37185.	1416.	-0.180E-05	-0.129E-05	-17.702	-17.831
37186.	1411.	-0.202E-05	-0.134E-05	-17.647	-17.779
37187.	1406.	-0.382E-05	-0.143E-05	-17.366	-17.499

TABLE II (cont.)

MJD	Z	$\dot{P}$(D)	$\dot{P}$(R)	LOG RHO H=0.200	LOG RHO H=0.400
37188.	1402.	-0.244E-06	-0.151E-05	-18.557	-18.692
37189.	1396.	-0.276E-05	-0.155E-05	-17.499	-17.635
37190.	1390.	-0.300E-05	-0.158E-05	-17.457	-17.595
37191.	1384.	-0.242E-05	-0.162E-05	-17.545	-17.685
37192.	1378.	-0.386E-05	-0.165E-05	-17.337	-17.479
37193.	1373.	-0.247E-05	-0.170E-05	-17.526	-17.669
37194.	1367.	-0.354E-05	-0.171E-05	-17.366	-17.510
37195.	1362.	-0.310E-05	-0.174E-05	-17.419	-17.565
37196.	1355.	-0.337E-05	-0.174E-05	-17.376	-17.524
37197.	1349.	-0.230E-05	-0.173E-05	-17.537	-17.686
37198.	1345.	-0.468E-05	-0.177E-05	-17.226	-17.376
37199.	1339.	-0.374E-05	-0.177E-05	-17.318	-17.470
37200.	1333.	-0.378E-05	-0.173E-05	-17.308	-17.462
37201.	1327.	-0.315E-05	-0.168E-05	-17.383	-17.538
37202.	1322.	-0.280E-05	-0.163E-05	-17.431	-17.587
37203.	1316.	-0.636E-05	-0.156E-05	-17.070	-17.228
37204.	1312.	-0.388E-05	-0.149E-05	-17.282	-17.440
37205.	1306.	-0.927E-06	-0.136E-05	-17.899	-18.059
37206.	1301.	-0.294E-05	-0.122E-05	-17.394	-17.555
37207.	1296.	-0.163E-05	-0.105E-05	-17.646	-17.808
37208.	1291.	-0.409E-05	-0.878E-06	-17.244	-17.407
37209.	1287.	-0.453E-05	-0.710E-06	-17.197	-17.361
37210.	1282.	-0.172E-05	-0.565E-06	-17.615	-17.779
37211.	1278.	-0.313E-05	-0.497E-06	-17.353	-17.517
37212.	1273.	-0.258E-05	-0.506E-06	-17.433	-17.598
37213.	1270.	-0.436E-05	-0.607E-06	-17.203	-17.369
37214.	1266.	-0.409E-05	-0.748E-06	-17.230	-17.396
37215.	1262.	-0.206E-05	-0.896E-06	-17.526	-17.693
37216.	1260.	-0.284E-05	-0.105E-05	-17.385	-17.552
37217.	1257.	-0.378E-05	-0.119E-05	-17.260	-17.427
37218.	1253.	-0.365E-05	-0.132E-05	-17.274	-17.442
37219.	1251.	-0.353E-05	-0.144E-05	-17.288	-17.456

TABLE II (cont.)

MJD	Z	$\dot{P}$(D)	$\dot{P}$(R)	LOG RHO H=0.200	LOG RHO H=0.400
37220.	1248.	-0.271E-05	-0.145E-05	-17.403	-17.570
37221.	1245.	-0.361E-05	-0.162E-05	-17.277	-17.445
37222.	1242.	-0.353E-05	-0.170E-05	-17.286	-17.454
37223.	1240.	-0.452E-05	-0.178E-05	-17.179	-17.346
37224.	1235.	-0.339E-05	-0.184E-05	-17.303	-17.470
37225.	1232.	-0.426E-05	-0.191E-05	-17.204	-17.371
37226.	1230.	-0.497E-05	-0.200E-05	-17.136	-17.303
37227.	1226.	-0.330E-05	-0.206E-05	-17.313	-17.479
37228.	1222.	-0.336E-05	-0.213E-05	-17.304	-17.471
37229.	1219.	-0.315E-05	-0.221E-05	-17.334	-17.500
37230.	1216.	-0.225E-05	-0.229E-05	-17.479	-17.645
37231.	1214.	-0.189E-05	-0.239E-05	-17.554	-17.720
37232.	1213.	-0.260E-05	-0.249E-05	-17.417	-17.582
37233.	1207.	-0.309E-05	-0.252E-05	-17.341	-17.506
37234.	1205.	-0.153E-05	-0.262E-05	-17.646	-17.811
37235.	1201.	-0.845E-05	-0.267E-05	-16.904	-17.068
37236.	1192.	-0.486E-05	-0.264E-05	-17.141	-17.305
37237.	1187.	-0.118E-05	-0.270E-05	-17.754	-17.919
37238.	1189.	-0.116E-05	-0.285E-05	-17.763	-17.927
37239.	1181.	-0.238E-05	-0.284E-05	-17.449	-17.614
37240.	1177.	-0.233E-05	-0.289E-05	-17.457	-17.621
37241.	1173.	-0.349E-05	-0.293E-05	-17.280	-17.445
37242.	1168.	-0.375E-05	-0.294E-05	-17.248	-17.412
37243.	1163.	-0.339E-05	-0.295E-05	-17.290	-17.454
37244.	1157.	-0.331E-05	-0.294E-05	-17.299	-17.464
37245.	1153.	-0.361E-05	-0.294E-05	-17.259	-17.425
37246.	1148.	-0.414E-05	-0.295E-05	-17.199	-17.364
37247.	1143.	-0.134E-05	-0.293E-05	-17.685	-17.851
37248.	1137.	-0.272E-05	-0.290E-05	-17.377	-17.543
37249.	1132.	-0.473E-05	-0.288E-05	-17.134	-17.301
37250.	1126.	-0.503E-05	-0.285E-05	-17.106	-17.272
37251.	1121.	-0.920E-05	-0.282E-05	-16.842	-17.008

TABLE II (cont.)

MJD	Z	$\dot{P}$(D)	$\dot{P}$(R)	LOG RHO H=0.200	LOG RHO H=0.400
37252.	1119.	-0.850E-05	-0.285E-05	-16.876	-17.043
37253.	1113.	-0.508E-06	-0.283E-05	-18.097	-18.265
37254.	1106.	-0.487E-05	-0.278E-05	-17.112	-17.280
37255.	1100.	-0.444E-05	-0.277E-05	-17.151	-17.319
37256.	1100.	-0.237E-05	-0.283E-05	-17.423	-17.591
37257.	1093.	-0.519E-05	-0.281E-05	-17.080	-17.249
37258.	1086.	-0.236E-05	-0.280E-05	-17.420	-17.588
37259.	1082.	-0.373E-05	-0.280E-05	-17.220	-17.389
37260.	1077.	-0.461E-05	-0.286E-05	-17.127	-17.296
37261.	1073.	-0.310E-05	-0.290E-05	-17.297	-17.467
37262.	1068.	-0.305E-05	-0.295E-05	-17.304	-17.473
37263.	1065.	-0.403E-05	-0.303E-05	-17.182	-17.351
37264.	1060.	-0.265E-05	-0.309E-05	-17.364	-17.533
37265.	1056.	-0.364E-05	-0.315E-05	-17.224	-17.394
37266.	1051.	-0.331E-05	-0.322E-05	-17.265	-17.435
37267.	1047.	-0.415E-05	-0.331E-05	-17.166	-17.336
37268.	1043.	-0.273E-05	-0.340E-05	-17.348	-17.517
37269.	1038.	-0.572E-05	-0.347E-05	-17.026	-17.195
37270.	1034.	-0.550E-05	-0.355E-05	-17.043	-17.212
37271.	1026.	-0.357E-05	-0.361E-05	-17.229	-17.398
37272.	1022.	-0.696E-05	-0.369E-05	-16.939	-17.107
37273.	1019.	-0.630E-05	-0.381E-05	-16.983	-17.151
37274.	1017.	-0.486E-05	-0.392E-05	-17.096	-17.264
37275.	1012.	-0.506E-05	-0.398E-05	-17.079	-17.246
37276.	1008.	-0.766E-05	-0.404E-05	-16.899	-17.066
37277.	1004.	-0.734E-05	-0.409E-05	-16.918	-17.085
37278.	1002.	-0.647E-05	-0.416E-05	-16.974	-17.141
37279.	995.	-0.427E-05	-0.410E-05	-17.154	-17.320
37280.	991.	-0.629E-05	-0.407E-05	-16.986	-17.152
37281.	982.	-0.805E-05	-0.390E-05	-16.878	-17.043
37282.	983.	-0.506E-05	-0.383E-05	-17.081	-17.246
37283.	979.	-0.597E-05	-0.359E-05	-17.010	-17.175

TABLE II (cont.)

MJD	Z	$\dot{P}$(D)	$\dot{P}$(R)	LOG RHO H=0.200	LOG RHO H=0.400
37284.	975.	-0.697E-05	-0.324E-05	-16.942	-17.106
37285.	969.	-0.664E-05	-0.264E-05	-16.962	-17.126
37286.	966.	-0.477E-05	-0.133E-05	-17.106	-17.269
37287.	963.	-0.501E-05	-0.278E-07	-17.084	-17.247
37288.	959.	-0.488E-05	-0.286E-07	-17.095	-17.258
37289.	956.	-0.515E-05	-0.228E-07	-17.071	-17.234
37290.	954.	-0.488E-05	-0.273E-07	-17.094	-17.257
37291.	951.	-0.370E-05	-0.144E-07	-17.214	-17.377
37292.	949.	-0.343E-05	-0.132E-07	-17.246	-17.408
37293.	947.	-0.396E-05	-0.125E-07	-17.183	-17.346
37294.	945.	-0.414E-05	-0.245E-08	-17.163	-17.325
37295.	944.	-0.424E-05	-0.136E-08	-17.153	-17.315
37296.	943.	-0.560E-05	-0.338E-09	-17.032	-17.194
37297.	943.	-0.490E-05	-0.299E-09	-17.090	-17.252
37298.	943.	-0.490E-05	-0.307E-09	-17.089	-17.252
37299.	943.	-0.569E-05	-0.356E-08	-17.024	-17.187
37300.	944.	-0.550E-05	-0.516E-08	-17.039	-17.202
37301.	944.	-0.545E-05	-0.773E-08	-17.043	-17.206
37302.	946.	-0.533E-05	-0.135E-07	-17.052	-17.215
37303.	947.	-0.541E-05	-0.138E-07	-17.046	-17.209
37304.	949.	-0.518E-05	-0.211E-07	-17.065	-17.229
37305.	951.	-0.514E-05	-0.289E-07	-17.068	-17.232
37306.	954.	-0.509E-05	0.483E-06	-17.073	-17.237
37307.	956.	-0.526E-05	0.150E-05	-17.058	-17.223
37308.	958.	-0.508E-05	0.194E-05	-17.073	-17.238
37309.	960.	-0.407E-05	0.219E-05	-17.170	-17.336
37310.	960.	-0.335E-05	0.230E-05	-17.254	-17.420